Development of a Six-Axis Force and Torque Sensor for the Humanoid Robot Sweaty 2.0

Lucas Schickl, Klaus Dorer, Michael Wülker, Yuri D'Antilio and Ulrich Hochberg
University of Applied Science Offenburg, Germany

***Abstract*— The humanoid Sweaty was the finalist in this year's robocup soccer championship(adult size). For the optimization of the gait and the stability, data concerning forces and torques in the ankle joints would be helpful. In the following paper the development of a six-axis force and torque sensor for the humanoid robot Sweaty is described. Since commercial sensors do not meet the demands for the sensors in Sweatys ankle joints, a new sensor was developed. As a measuring devices we used strain gauges and custom electronics based on an *acam* PS09. The geometry was analyzed with the FEM program *ANSYS* to get optimal dimensions for the measuring beams. In addition *ANSYS* was used to optimize the position for the strain gauges on the beam.**

I. INTRODUCTION

An objective for two legged humanoid robots, particularly in soccer playing, is dynamic walking. In this case it is necessary to have sensors, which help to stabilize the robot during its movement. Therefore different sensing technologies for dynamic and stable walking were analyzed. Based on this analysis, a six-axis force and torque sensor (F/T sensor) was developed, which fits into limited space, is as light weighted as possible and is also economic. The sensor detects the forces and moments along all space coordinates.

The gathered forces and moments can be used to determine the *Zero Moment Point* (ZMP) and the *Center of Pressure* (CoP). The ZMP can be used to achieve stable walking, while it is used to find the point, where all moments of tilt are zero. As long as the ZMP of the robot is inside the support polygon, the robot will not fall. With the help of this information it is possible to reach higher walking speed and eventually dynamic walking with Sweaty (Fig. 1).

Fig. 1. *Sweaty 2.0*

II. RELATED WORK

There are different sensing technologies used to measure contact forces and torqures for humanoid robots. The robot NAO from the company *SoftBank Robotics* uses four Force Sensitive Resistances (FSR) [1] in each foot. These FSR sensors are only detecting pressure and have poor resolution, but they are quite cheap and are easy to integrate into a robot (Fig. 3).

The concept of a F/T sensor is well known. Many different F/T sensors are commercially available. They are often used for industrial robots where weight and size is not as important as it is for humanoid robots. But there are already some robots with F/T senors implemented, like *ASIMO* from *Honda* [2] and *HRP4* from *KAWADA INDUSTRIES,Inc.* [3]. Scheinmann et. al developed a *Maltese cross* sensor. This sensor was improved for space applications [4] [5]. Yuan [6] optimized the sensor for feet of humanoid robots. For Sweaty's feet, the design had to be adopted and modified. The electronics had to be simplified and the weight had to be reduced. In addition the electronics had to be integrated into the sensor and a communication via CAN had to be established.

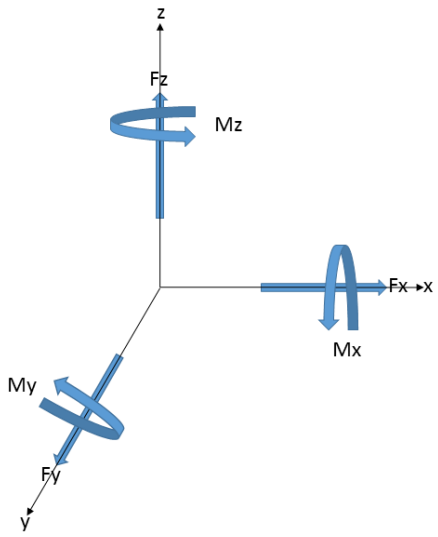

Fig. 2. Spatial components of force and torque

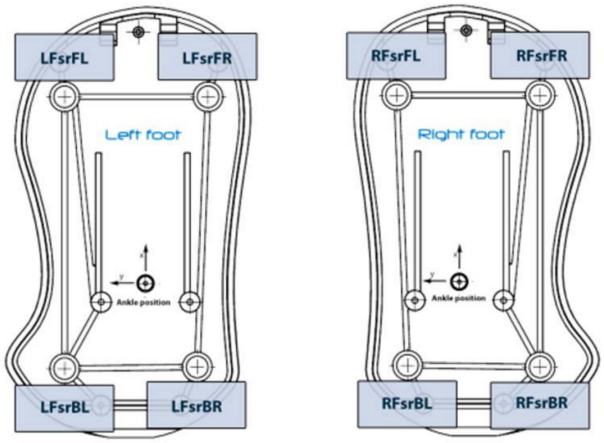

Fig. 3. FSR placed on the feet from a NAO robot [1]

III. GEOMETRY OF THE SENSOR

From the analysis of different scientific work about six-axis sensors, our sensors geometry bases on a *Maltese* cross which connects an inner to an outer flange (Fig. 4). This links the flanges with four beams. This concept is similar to the one Chao Yuan [6] and colleagues had investigated. Based on their work, a sensor geometry was designed for Sweaty's feet under the aspect of the required forces and torques, low weight, small dimensions and adjusted electronics. The geometry was chosen because it is simple to manufacture with common tools and it fits well between the foot and the ankle of the robot.

Every beam of the *Maltese cross* is equipped with four strain gauges, which are measuring the bending of the beams. To prevent the strain gauges from reacting to elongation each beam ends in an elastic membrane which is an integrated part

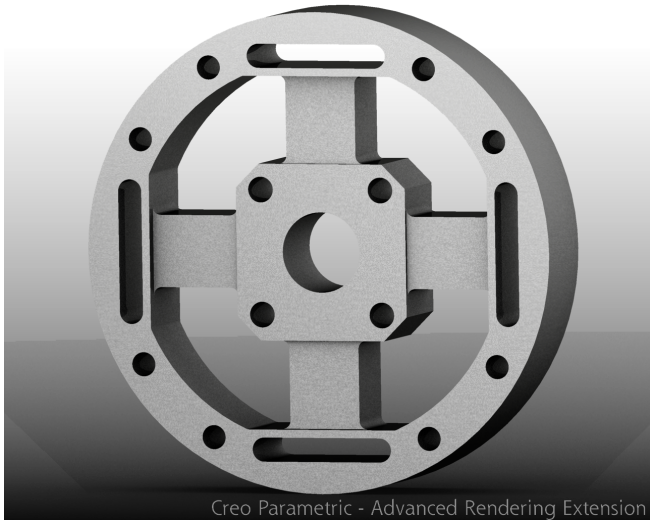

Fig. 4. Maltese cross geometry

of the aluminum structure and meant to compensate cross coupling errors. These errors occur if a force acts along one axis. The two beams orthogonal to the force will bend and the two along the force will experience elongation. If the geometry has an elastic membrane, it will deform and absorb most of the elongation from the beams and the signal of the bend beams is much stronger than the signal from the strain gauges of the elongated beams.

IV. FEM ANALYSIS

A. Material

After the geometry was chosen, a material had to be selected. The material should have a high yield limit, to sustain the high loads. Table I shows the values we got from the actuators from the robot and from simulation data.

TABLE I
MAXIMUM LOAD

Fx	800 N	Tx	50 Nm
Fy	800 N	Ty	50 Nm
Fz	2100 N	Tz	50 Nm

One option was the steel alloy 1.6580 (30CrNiMo8) which has a yield strength of 1050 MPa and the other one was an EN AW 7075 T651 aluminum alloy with a yield strength of 460 MPa to 470 MPa. As the results of the FEM analysis has given us a maximum stress of 346,96 MPa (Fig. 5, 6), the aluminum alloy has enough reliability to be used safely. As the steel alloy is very ductile and difficult to process by cutting it was preferred to choose the aluminum.

B. Positioning of the strain gauges

For the best position of the strain gauges another simulation was performed. Virtual strain gauges were placed on the surface of the 3D model (Fig. 7). The virtual strain gauge can be seen as ideal elastic material and has a thickness near to zero.

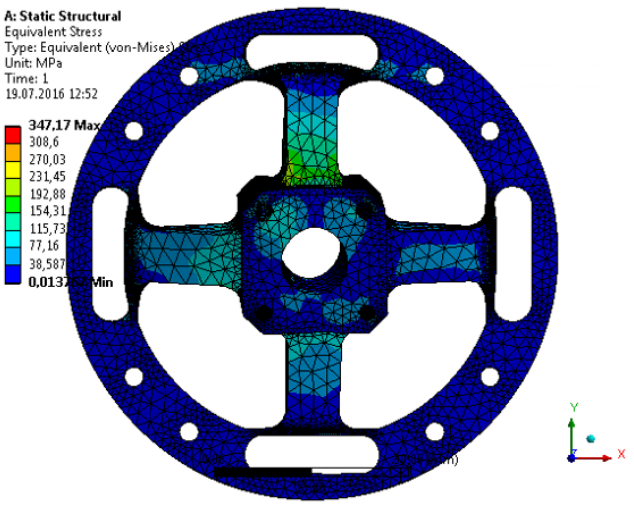

Fig. 5. Result from FEM analysis with Equivalent Stress Method (von-Mises)

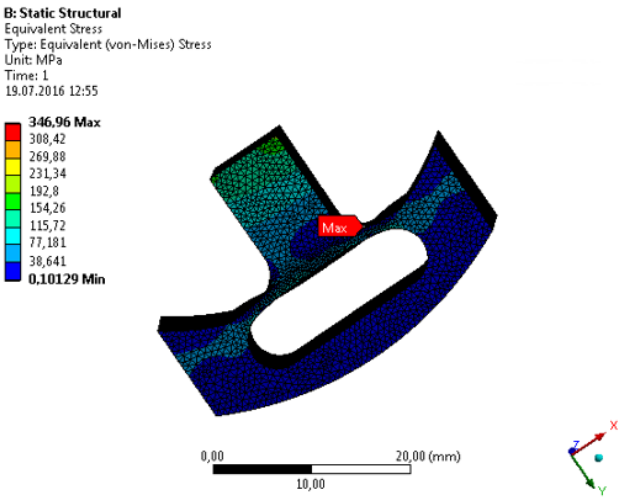

Fig. 6. Sub model with finer mesh for more details

The strain gauges where placed in different positions measured from the center. Table II shows the results of the simulation.

Position one, 12.95mm, is the nearest possible position, where the strain gauge gets in contact with the radius from the manufacturing. The higher the results of the ϵ_{min} value is, the better is the position. As the chosen strain gauges from the company *HBM* have a minimum detection value of 0.1 $\frac{\mu m}{m}$, the first position at 12.95mm was selected.

V. ELECTRONICS

The 16 strain gauges are connected to eight half bridges which are connected to a specially developed electronic board based on an *acam* PS09 [7]. As a PS09 chip can only handle four half bridges, two of them are needed.

Figure 8 shows the locations of the strain gauges on the sensor geometry, while Table III shows how they are connected.

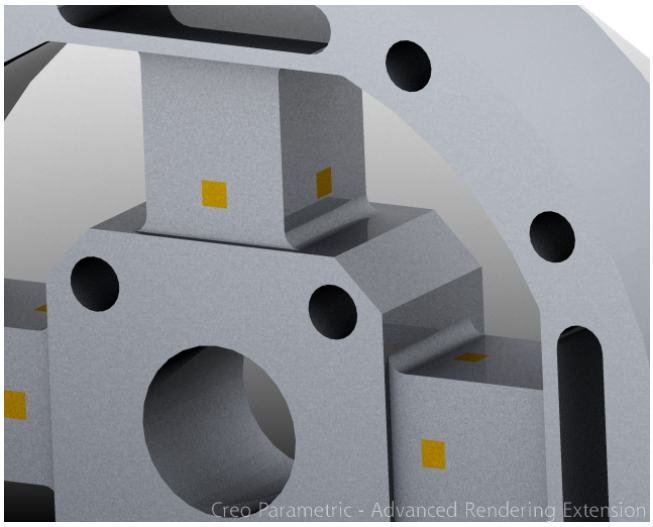

Fig. 7. Virtual stain gauges

TABLE II

MINIMUM VALUES OF THE DEFORMATION OBTAINED PLACING STRAIN GAUGES AT DIFFERENT DISTANCES FROM THE CENTER OF THE SENSOR.

Distances from the center [mm]	$\epsilon_{min}\,\frac{\mu m}{m}$
12.95	0.52546
13.95	0.44532
14.95	0.37010
15.95	0.29516

In table III z_1 to z_8 are the eight half bridges, from which the *acam* PS09 gathers its values.

Figure 10 shows how the four half bridges are connected to the PS09. The relative change of the resistances is not measured directly but using measuring times of loading a capacitor. As time can be measured relatively easy, the sensor has a relatively high accuracy though only a few external components are needed.

From this scheme the electronics was designed. This resulted in a small electronic board with two PS09 chips (Fig. 11), which are measuring the bending of the beams and send the data to a custom controller (Fig. 12) where they are filtered and multiplied with the calibration matrix. The controller than sends the calculated forces and torques to the main PC of the robot via CAN-bus.

TABLE III

BRIDGE CIRCUIT

Bridge Circuit	Strain gauges number
z_1	$(\epsilon_{11} - \epsilon_{15})$
z_2	$(\epsilon_{10} - \epsilon_{14})$
z_3	$(\epsilon_7 - \epsilon_6)$
z_4	$(\epsilon_4 - \epsilon_8)$
z_5	$(\epsilon_1 - \epsilon_5)$
z_6	$(\epsilon_{13} - \epsilon_{16})$
z_7	$(\epsilon_2 - \epsilon_3)$
z_8	$(\epsilon_{12} - \epsilon_9)$

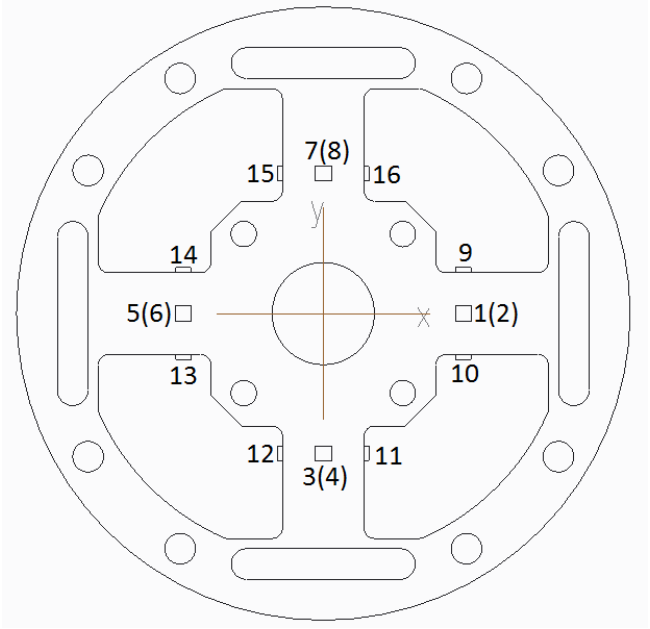

Fig. 8. Placement of the strain gauges

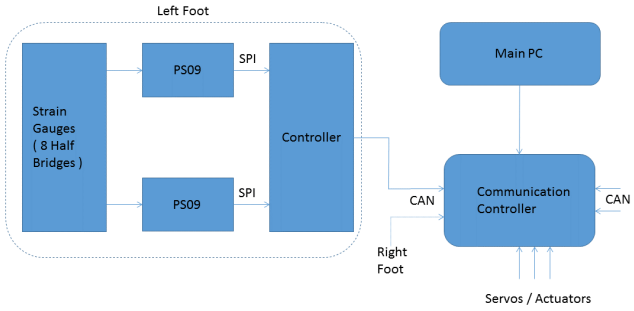

Fig. 9. Schematic view of the working principal for the electronics

VI. TEST AND CALIBRATION

For testing and calibration of the sensor, a test bench was build (Fig. 13), which uses an F/T-sensor from *ATI Industrial Automation* [8] as reference. The *ATI* sensor is placed on a plate, which is connected to a table. The top of the *ATI* sensor carries an adapter for the new sensor, where it is connected over the outer flange. The inner flange is connected to a profile that ends in a top plate with holes inside.

The data gathered from both sensors are collected in data files from which they can be used for calibration. It was necessary to collect several load points with different forces and torques. To get a torque along the Z axis a cable system was used.

After the readings from both instruments were registered, the values were used to calculate calibration matrix *C*, which is a 6x8 matrix. For the calibration the *least square method* [3] was used. Finally the vector for the forces and torques can be calculated by

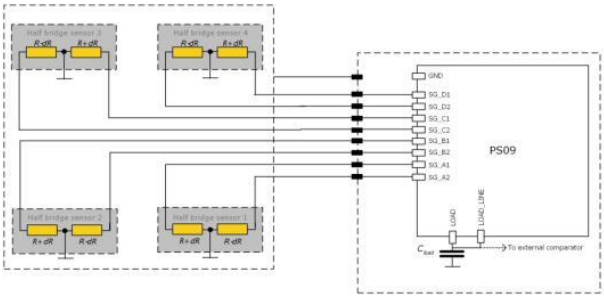

Fig. 10. PS09 configuration with 4 half bridges [7]

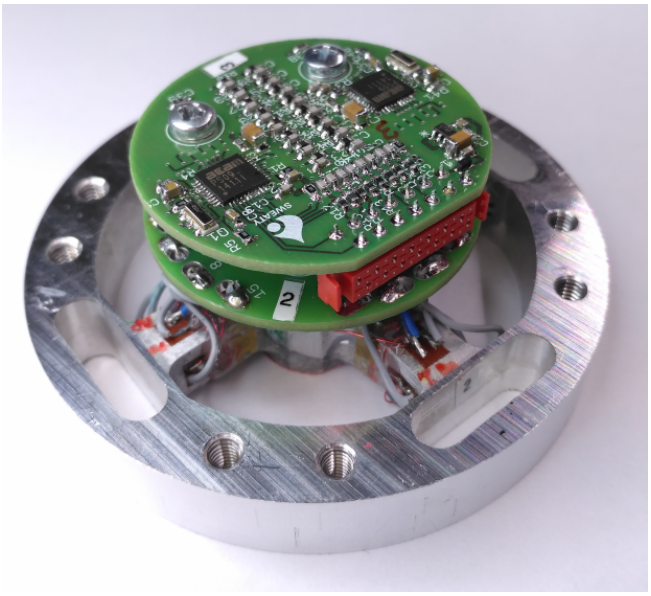

Fig. 11. PS09 board attached to the sensor geometry

$$\begin{bmatrix} F_x \\ F_y \\ F_z \\ T_x \\ T_y \\ T_z \end{bmatrix} = C \begin{bmatrix} z_1 \\ z_2 \\ z_3 \\ z_4 \\ z_5 \\ z_6 \\ z_7 \\ z_8 \end{bmatrix}. \quad (1)$$

where z_1 to z_8 are the signals from the half bridges.

The forces and torques are measured with a frequency of 800Hz and the average data is transmitted with a frequency of 100Hz. The average figures show a standard deviation of 1N for forces and 0.1Nm for torques. Figure 15 shows the raw sensor data over time during calibration of one sensor. Typically we used 100 measurements for the calibration on each load case. The standard deviation of the raw signal is about 300-600, while the raw sensor data have a scale up to 10^5 depending on the local case. The total measurement range is 10^6.

Table IV shows the measured values from the *ATI* sensor and the values gathered from the 6x8 matrix. The load

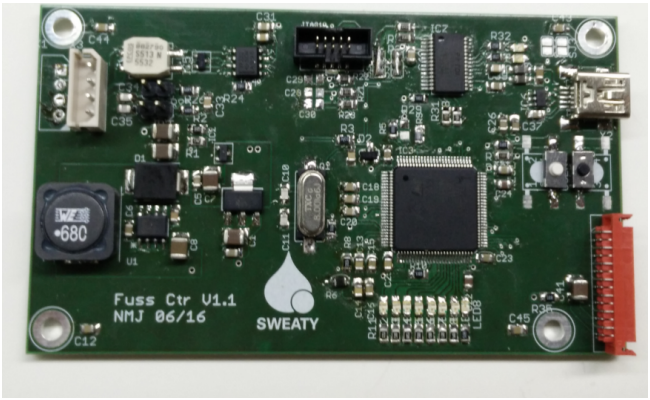

Fig. 12. Controller board for the foot

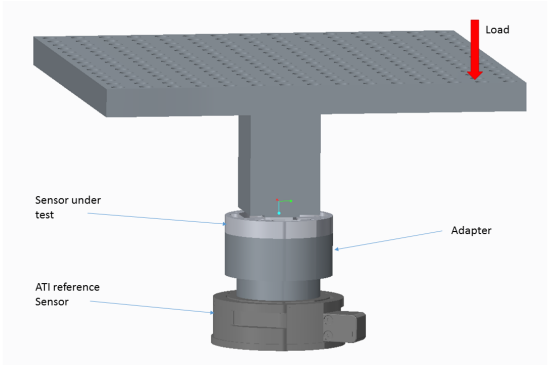

Fig. 13. Test bench with reference sensor and sensor under investigation

cases 1-5 represents typical positions for the center of mass projection onto the foot of *Sweaty*. Load case 6-11 were done to achieve decoupled signals from F_x,F_y and T_z. For further improvements we want to refine the calibration matrix. As the existing matrix has only 11 load cases the results are already good, but with more load cases the results should even get better.

VII. CONCLUSION AND FUTURE WORK

A new foot force sensor has been developed. By modifying the idea of a *Maltese cross* sensor using an integrated circuit based on time measurements, the weight of the sensor could be reduced dramatically. The introduction of a 6x8 matrix was helpful to calculate the forces and torques.

Sweaty's future foot will include a force and torque sensor which is lightweight and includes the electronics. The total weight of the sensor, electronics and cable is 134 g. There is the possibility to reduce the weight of the electronics by modifying the PCB in further revisions, but the decrease in weight might be slight. The additional information gathered from the sensors in the feet will help to stabilize Sweaty's gait.

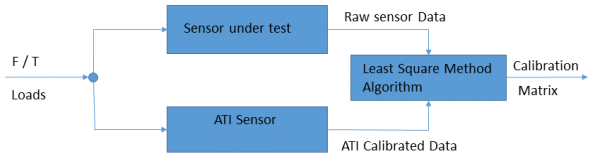

Fig. 14. Flow chart of the configuration

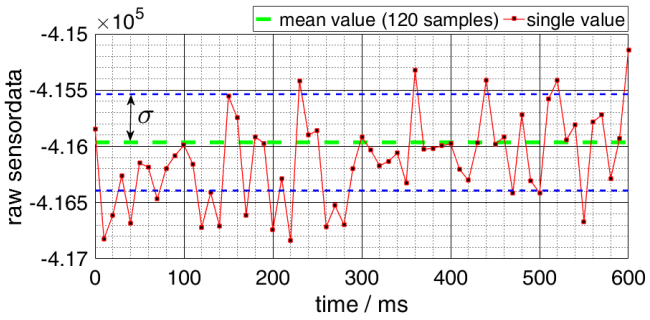

Fig. 15. Raw sensor data for load case1 with mean value and standard deviation.

TABLE IV
LOAD CASES FROM ATI SENSOR AND BACK CALCULATED VALUES WITH 6X8 MATRIX

load case	F_x / N	F_y / N	F_z / N	T_x / Nm	T_y / Nm	T_z / Nm
1 meas.	-1.2	0.9	-168.8	-0.8	-23.8	-0.1
1 calc.	-0.7	0.3	-169.6	-0.8	-23.9	-0.1
2 meas.	0.1	3.2	-167.4	-23.6	0.0	0.1
2 calc.	0.3	3.0	-167.5	-23.6	0.0	0.1
3 meas.	1.6	1.5	-165.9	0.5	23.4	0.1
3 calc.	2.1	1.0	-166.8	0.5	23.3	0.1
4 meas.	-0.9	-1.6	-167.9	23.4	-0.4	-0.1
4 calc.	-0.8	-1.8	-167.9	23.4	-0.4	-0.1
5 meas.	0.2	1.4	-167.6	-0.0	-0.1	-0.0
5 calc.	-1.1	2.8	-165.8	-0.0	-0.1	0.0
6 meas.	0.9	0.2	0.3	-0.0	0.1	12.6
6 calc.	0.2	1.1	0.1	-0.0	0.1	12.6
7 meas.	0.2	-0.5	0.4	0.1	0.1	-12.2
7 calc.	-0.5	0.5	0.1	0.1	0.1	-12.2
8 meas.	0.1	-49.4	0.2	0.7	0.0	0.1
8 calc.	0.2	-49.7	-0.8	0.7	0.0	0.1
9 meas.	0.0	49.6	0.4	-0.7	-0.0	0.0
9 calc.	0.3	49.2	-0.5	-0.7	-0.0	0.0
10 meas.	49.0	0.0	0.6	-0.1	0.7	0.0
10 calc.	48.6	0.9	0.0	-0.1	0.7	0.0
11 meas.	-49.2	-0.0	-0.2	-0.0	-0.7	0.1
11 calc.	-49.6	0.8	-0.8	0.0	-0.7	0.1

ACKNOWLEDGMENT

The authors would like to thank the University of Applied Science Offenburg for the support of the project as well as Becker & Müller Schaltungsdruck GmbH for their sponsorship.

REFERENCES

[1] "Softbank robotics europe:force sensitive resistance," 2014. [Online]. Available: http://doc.aldebaran.com/2-1/family/robots/fsr_robot.html
[2] "Honda motor co.: Honda asimo - technical information," 2007. [Online]. Available: http://asimo.honda.com/downloads/pdf/asimo-technical-information.pdf
[3] B. D. and W. H., "Techniques for robotic force sensor calibration," *Proceedings fo the 13th International Workshop on Computer Science and Information Technologies CSIT'2011*, pp. 218–2237, 2011.

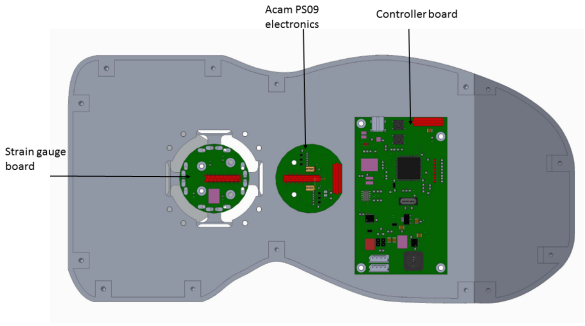

Fig. 16. Bottom view of *Sweaty*'s foot with arrangement of the electronics.

[4] D. Chen, A. Song, and A. Li, "Design and calibration of a six-axis force/torque sensor with large measurement range used for the space manipulator," *Procedia Engineering*, vol. 99, pp. 1164 – 1170, 2015. [Online]. Available: http://www.sciencedirect.com/science/article/pii/S1877705814038168

[5] Y. Sun, Y. Liu, T. Zou, M. Jin, and H. Liu, "Design and optimization of a novel six-axis force/torque sensor for space robot," *Measurement*, vol. 65, pp. 135 – 148, 2015. [Online]. Available: http://www.sciencedirect.com/science/article/pii/S0263224115000238

[6] C. Yuan, L.-P. Luo, Q. Yuan, J. Wu, R.-J. Yan, H. Kim, K.-S. Shin, and C.-S. Han, "Development and evaluation of a compact 6-axis force/moment sensor with a serial structure for the humanoid robot foot," *Measurement*, vol. 70, pp. 110 – 122, 2015. [Online]. Available: http://www.sciencedirect.com/science/article/pii/S0263224115001736

[7] acam Messelektronik GmbH, "Datasheet ps9, vol. 1," pp. 3–6, 2014.

[8] A. I. Automation, "Si-660-60," 2005. [Online]. Available: http://www.ati-ia.com/library/documents/ATI_FT_Sensor_Catalog_2005.pdf

Fig. 17. Sweaty's new and Sweaty's old foot